The Kinetics of O_2 Reduction Studies on Hyperstoichiometric $UO_{2.002}$ Electrode

Heming He, J.J. Noel and D.W. Shoesmith
Department of Chemistry
The University of Western Ontario

Abstract

The cathodic reduction of O_2 is one of the major reactions involved in nuclear fuel corrosion under permanent waste disposal conditions. The kinetics of this reaction have been studied in dilute alkaline aqueous solution on a slightly hyperstoichiometric $UO_{2.002}$ electrode using rotating disc techniques. Overall, a four electron reduction to OH^- with a reaction order of one with respect to O_2 has been observed under these conditions. However once blockage of active sites occurs by adsorption or surface oxidation, the O_2 reduction reaction may deviate from the four-electron process.

Keywords: Hyperstoichiometry, UO_2, O_2 reduction, Reaction mechanism

1. INTRODUCTION

One Canadian option, for deep geologic disposal of nuclear wastes, which consist of uranium dioxide (UO_2) fuel, is to bury the spent fuel in copper containers 500-1000 m deep in the granitic rock of the Canadian Shield[1]. The rate of release of radionuclides from spent fuel once it comes in contact with groundwater is the source term for performance assessment of this concept. Most radionuclides (>95%) are retained in the grains of the sintered UO_2 pellets and will not be released until the solid matrix dissolves. Consequently, their release will be governed primarily by the corrosion kinetics of the UO_2 matrix.

The most important parameter in determining fuel corrosion rates is the redox condition inside a failed waste container. Previous studies show UO_2 has extremely limited solubility and a very low dissolution rate under reducing conditions, but the solubility increases greatly under oxidizing conditions[2]. Generally, reducing conditions can be expected in a nuclear waste repository, but radiolytic decomposition of water will generate various oxidants (e.g. O_2, O_2^-, OH and H_2O_2) near the surface of the fuel. Hence, once container failure occurs the UO_2 surfaces could be subject to an oxidizing environment for long periods of time.

The importance of cathodic oxygen reduction in the corrosion of spent fuel has been previously discussed[3]. It is a potential oxidant that can drive fuel corrosion inside a failed waste container, since it can be produced directly by the alpha radiolysis of water or indirectly by the decomposition of alpha-radiolytically- produced H_2O_2,

$$2H_2O_2 \rightarrow O_2 + 2H_2O \cdots\cdots\cdots\cdots\cdots\cdots\cdots\cdots (1)$$

A recent study[4] indicates that one fuel parameter important in determining its reactivity may be the degree of non-stoichiometry in the UO_2 structure. Consequently, we are studying the kinetics of O_2 reduction on a range of UO_2 specimens of various degrees of non-stoichiometry. Here we present result obtained on a $UO_{2.002}$ specimen.

2. EXPERIMENTAL

2.1 Materials and Electrode Preparation

Experiments were performed on a well-characterized hyperstoichiometric $UO_{2.002}$ electrode. The hyperstoichiometric pellets, which were fabricated by Atomic Energy of Canada Limited (AECL) at Chalk River Laboratories (Ontario, Canada), were prepared by annealing ceramic UO_2 discs at high temperatures in various CO_2/CO gas mixtures.

the electrodes are approximately 3-5 mm thick and 12mm in diameter. One face of the disc was electroplated with a thin layer of Cu, which served as a good electrical contact; This Cu-plated surface was then glued to a stainless steel post with a highly conductive silver epoxy (Hysol KS004). The disc was then put into a casting compound (Hysol EE 4138, Wolcott-Park Incorporated), and allowed to solidify for 4 hours at 60 ºC, followed by 4 hours at 120ºC. The excess resin then removed from the electrode surface until a flat circular face of the electrode was exposed. Potentials were measured, and are quoted against, a saturated calomel electrode (SCE). The counter electrode was a ~ 10 cm^2 Pt sheet spot-welded to a Pt wire.

2.2 Solutions

All solutions were prepared using ultrapure distilled deionized water (18.2 MΩcm) purified using a Millipore-milli-Q plus unit to remove organic and inorganic impurities by passing through ion exchange columns. All chemicals were analytical grade. The solution pH was monitored with an Orion model 720A pH meter, and the pH adjusted with HCl or NaOH. All the solutions were 0.1 M NaCl, with some containing 0.025 M disodium tetraborate ($Na_2B_4O_7 \cdot 10H_2O$) and 0.025 M NaOH to buffer the pH to 9.5, and some without buffer with the pH adjusted to pH=9.5.

2.3 Electrochemical Cell and Equipment

All electrochemical experiments were performed in a three-electrode, there-compartment cell using a rotating disc electrode (RDE). The working electrode ($UO_{2.002}$) was attached to the shaft of a Pine Instruments model AFASR analytical rotator. Electrode rotation rates were varied from 0 to 33.3Hz. The electrochemical data was acquired with a Solartron 1287 potentiostat controlled by CoreWare^{TM} software. The current interrupt method was used to compensate for IR drop in the electrode.

2.4 Experimental Procedure

Prior to each experiment the electrode was polished (wet) with a 600grit SiC paper, rinsed with distilled deionized water, and re-polished (wet) with 1200 grit SiC paper. The electrode was then cathodically reduced in Ar- purged electrolyte at –1.7V for 5 minutes. O_2-reduction currents were recorded in air-purged electrolyte solutions by scanning from negative to positive potentials to avoid the influence of surface oxidation. The background currents recorded in Ar-purged solution, were used to correct for the influence of water reduction.

3 RESULTS AND DISCUSSION

3.1 Kinetics of oxygen reduction on $UO_{2.002}$

The O_2 reduction reaction can be used to probe the structure/ composition of the UO_2 surface. According to the theory of Presnov and Trunov[5] for O_2 reduction on p-type semiconductors, O_2 reduction could be catalyzed by $U^{IV}-U^{V}$ mixed oxidation states in the UO_2 surface, which act as an electron donor-acceptor relay system. Thus, a $U^{IV}_{1-2x}U^{V}_{2x}O_{2+x}$ surface would be expected to catalyze O_2 reduction. Under these conditions U^{V} in the electrode surface would accept an electron from the bulk and donate it to an O_2 molecule adsorbed under Langmuir conditions[6].

Oxygen reduction can proceed primarily via two pathways[7]:

(i) A four-electron reduction reaction without the formation of H_2O_2;

(ii) An initial reduction reaction producing H_2O_2, which is possibly then electroreduced to OH^- via the reaction.

$$O_2 + 2H_2O + 4e^- \rightarrow 4OH^- \cdots\cdots\cdots\cdots\cdots\cdots (2)$$
$$O_2 + H_2O + 2e^- \rightarrow HO_2^- + OH^- \cdots\cdots\cdots\cdots (3)$$
$$HO_2^- + H_2O + 2e^- \rightarrow 3OH^- \cdots\cdots\cdots\cdots\cdots\cdots (4)$$

It is also possible for H_2O_2 be formed as a stable product and not further reduced by reaction 4. Thus, there is the possibility for both a full $4e^-$ reduction and a $2e^-$ reduction. A rotating disk electrode (RDE) technique has been used to investigate the kinetics and mechanism of oxygen reduction on $UO_{2.002}$ electrode.

3.2 Polarization curves of O_2 reduction

The UO_2 electrode was placed in an Ar-purged electrolyte, and after cathodic cleaning at -1.7V for 5minutes, a cyclic voltammogram was recorded to obtain the background current for oxidation and reduction of the electrode. The electrode was then cathodically cleaned again and immediately placed in an Air (or O_2)-saturated electrolyte, and a polarization curve for O_2 reduction recorded at a sweep rate of 5mV/s.

Fig.1 shows the voltammograms for $UO_{2.002}$ recorded in Ar-purged and Air-saturated 0.1M NaCl-Borate buffer solution (pH=9.5) at 16.7Hz. When the voltammogram in an Ar-purged solution was subtracted from that in an Air-purged solution, the polarization curve for O_2 reduction is obtained, Fig.1.

Fig.2 shows a series of polarization curves (corrected for the background currents as in Fig.1) for O_2 reduction for the electrode rotation range from 4.17 to 33.33Hz, in 0.1M NaCl solution (pH9.5). All the curves exhibit a well developed, rotation speed dependent, current plateau at high overpotentials (-1.1 to -1.3 vs. SCE).

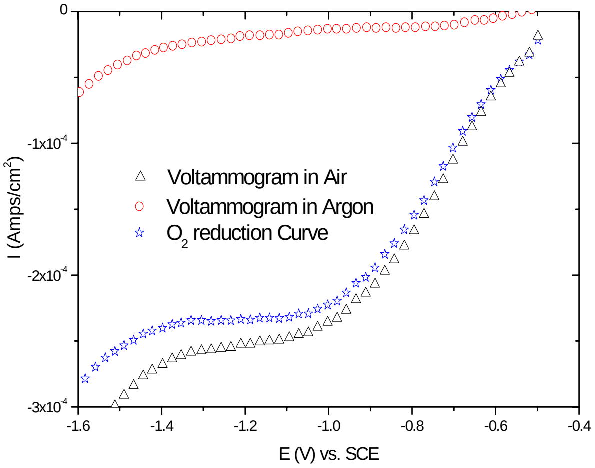

Fig.1 Voltammograms recorded on $UO_{2.002}$ in Ar- and Air-saturated 0.1MNaCl solution, and the polarization curve for O_2 reduction.

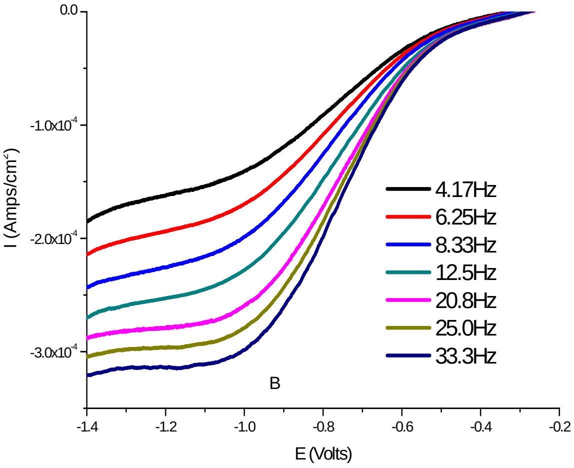

Fig.2 Cathodic-going polarization curves for O_2 reduction on $UO_{2.002}$, recorded in 0.1M NaCl at different electrode rotation rates. Sweep rate 5mV/s.

3.3 The O_2 reduction pathway

The rotation rate dependence of the plateau current densities (the limiting current, $\boldsymbol{i_L}$) indicates diffusion control, and $\boldsymbol{i_L}$ can be calculated using the Levich equation[8],

$$i_L = B\omega^{1/2} \cdots\cdots\cdots\cdots\cdots\cdots\cdots\cdots\cdots\cdots (5)$$

$$B = -0.62nFCD^{2/3}\gamma^{-1/6} \cdots\cdots\cdots\cdots\cdots (6)$$

Where $\boldsymbol{i_L}$ is the limiting current density, ***B*** is known as the transport parameter or Levich gradient, ***n*** is the number of electrons transferred per molecule of oxygen reduced, ***F*** is the Faraday constant (96500 C eq^{-1}), ***C*** is the bulk concentration of dissolved oxygen, ***D*** is the oxygen diffusion coefficient ($cm^2\ s^{-1}$) and ω is the electrode angular velocity (rad s^{-1}). Using a published set of values for oxygen reduction at 20ºC ($C = 2\times10^{-7} mol\ cm^{-3}$; $D = 1.9\times10^{-5} cm^2\ s^{-1}$; $\gamma = 0.0087 cm^2\ s^{-1}$)[9] $\boldsymbol{i_L}$ can be calculated yielding $B_{calc} = 68.8\times10^{-6} Acm^{-2}s^{-1}$ for a $4e^-$ reduction, and $B_{calc} = 34.4\times10^{-6} Acm^{-2}s^{-1}$ for a $2e^-$ reduction of O_2. The Levich equation gives a linear dependence of i_L on $\omega^{1/2}$ with a zero intercept and a slope proportional to the apparent number of electrons exchanged per O_2 molecule.

The plots of i_L vs. $\omega^{1/2}$ are shown in Fig.3 . The solid lines were calculated using eq. (6) for n=4 and n=2, the open circles and the solid stars are measured plateau currents with, and without borate

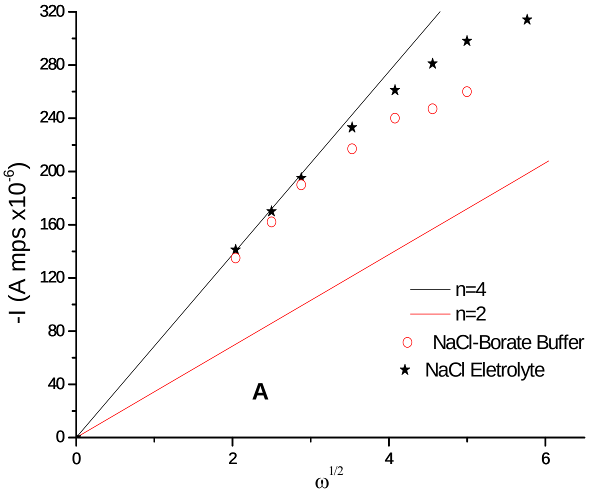

Fig.3 Levich plot for the O_2 reduction current on $UO_{2.002}$ RDE in Air-saturated 0.1M NaCl solution with buffer, and without buffer (pH9.5).Solid lines: Levich plots calculated for n=4 (black line) and n=2 (red line).

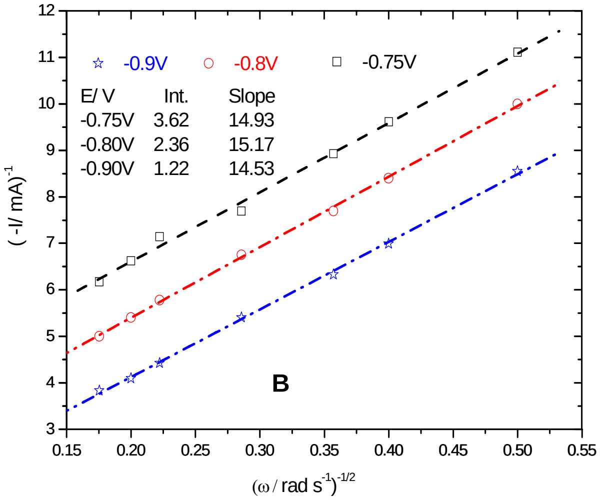

Fig4 Koutecky-Levich Plots for O_2 reduction on $UO_{2.002}$ in Air-purged 0.1M NaCl solution (pH=9.5). Data taken from Fig.2.

buffer. At low ω, O_2 reduction on the $UO_{2.002}$ electrode is a four-electron process, while at high ω, the reduction currents deviate from the n=4 plot. This indicates a kinetic limitation in addition to mass-transport[10]. Alternatively the production of a small amount of stable H_2O_2, a $2e^-$ process, could account for this deviation[11]. The slight difference in current with and without borate may suggest some involvement of the borate anion in the reduction process. A possibility is that some surface sites are blocked by its adsorption. Previous studies have shown that blockage of active sites on UO_2 by carbonate can lead to some H_2O_2 production[6].

Fig.4 shows plots of the data according to Koutecky-Levich equation.

$$\left(-\frac{1}{i}\right)^{1/m} = \left(-\frac{1}{i_{kin}}\right)^{1/m} + \frac{(-i)^{(1-\frac{1}{m})}}{B\omega^{1/2}} \cdots\cdots\cdots\cdots\cdots\cdots\cdots (7)$$

which, for the reaction order m=1, simplifies to:

$$\frac{1}{i} = \frac{1}{i_{kin}} + \frac{1}{B\omega^{1/2}} \cdots\cdots\cdots\cdots\cdots\cdots\cdots\cdots\cdots\cdots\cdots (7a)$$

The linearity and parallelism in these plots suggests the reaction is first order in O_2 for the three potentials.

The average experimental value of B is $B_{\exp} = 67.24 \times 10^{-6} Acm^{-2}s^{-1}$ (69.98×10^{-6}, 65.92×10^{-6}, and 68.82×10^{-6} respectively), which is very close to the theoretical value of 68.8×10^{-6} Acm^{-2} s^{-1} for a four-electron reduction. The non-zero intercept of the Koutecky-Levich plots shows there is a kinetic limitation to the current once the diffusion contribution is removed. This suggests that there may be a limitation in the number of active sites present on the surface of the electrode[12].

To more reliably determine the reaction order with respect to O_2, one has to vary the available concentration of oxygen in the vicinity of the electrode surface. This can be done in two ways. One is to vary the O_2 partial pressure in the gas phase and hence, the dissolved O_2 concentration in the solution, and the other is to vary the rotation rate of the electrode, which, for a constant applied potential, changes the O_2 concentration at the electrode surface, while in the bulk solution it remains unaltered.

For a series of values of $\boldsymbol{i}$ as a function of ω, this can be done by using equation (8),

$$\log(i) = \log(i_{kin}) + m \log(1 - \frac{i}{i_L}) \qquad (8)$$

Where i_{kin} is the current density corrected for diffusion effects, i and i_L are defined above. Equation (8) can be employed only when the reaction is under mixed activation-diffusion control (i.e., in the potential range from -0.65 to -0.95V in Fig.2). The values of i are taken from the polarization curves in Fig.2, and using the theoretical value of B (68.8×10^{-6} Acm^{-2} s^{-1}) to obtain i_L, equation (8) yields good straight lines with slopes of 1.02, 1.08, 1.07 respectively, as shown in Fig.5. These results confirm a first order reaction for O_2 reduction at potentials more negative then -0.6V. At more positive potentials, O_2 reduction is not significantly influenced by diffusion, and this analysis becomes inaccurate.

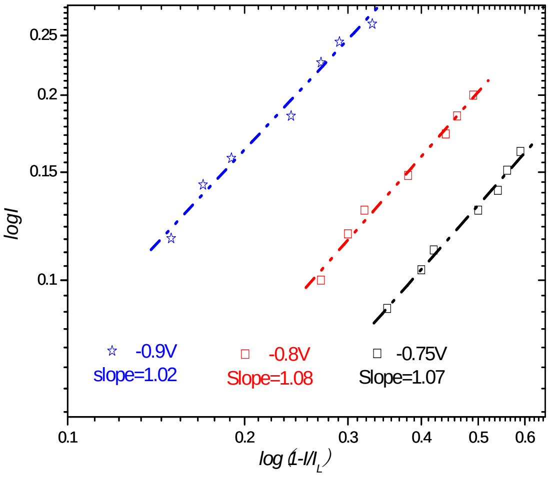

Fig.5 Determination of the reaction order with respect to O_2 reduction on $UO_{2.002}$ RDE in Air-Purged 0.1M NaCl solution (pH=9.5).

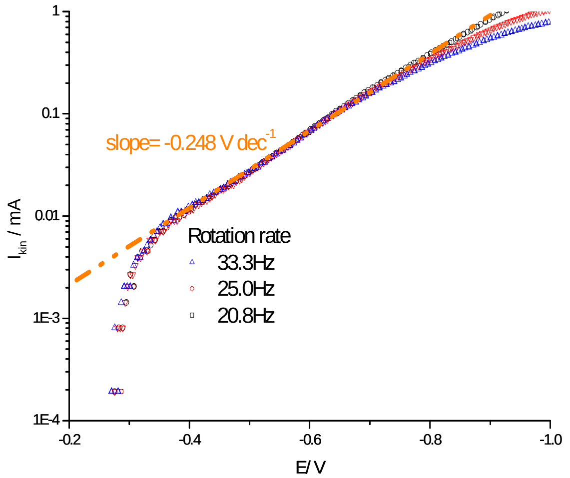

Fig.6 Tafel plots for O_2 reduction on $UO_{2.002}$ electrode. Data taken from Fig2

3.4 Tafel plots

The current plotted in Fig.2 were compensated for diffusion effects using eq. (8) over the entire potential range to yield the current free of diffusion effects, i_{kin}.

$$i_{kin} = \frac{i_L i}{i_L - i} \quad\text{.......................................}(9)$$

Fig.6 shows that $\log i_{kin}\ vs.\ E$ plots for different rotation rates in the potential range -0.35V to -0.95V overlap. The deviations from Tafel behaviour at high overpotentials may reflect difficulties in correcting the current for the onset of H_2O reduction.

For E>-0.4V the current will be influenced by electrode oxidation processes. For E< -0.4V, the Tafel slope is 0.248V dec^{-1}. The Tafel slope observed is consistent with values obtained in previous measurements on uncharacterized UO_2 electrodes[6], which ranged from 130mV dec^{-1} to 278mV dec^{-1}. The high values were attributed to a potential-dependence of the number of available active sites in the electrode surface. This suggests that at increasing negative potentials the number of available U^V sites is reduced.

4. SUMMARY AND CONCLUSIONS

The kinetics and mechanism of O_2 reduction have been studied on a $UO_{2.002}$ electrode and shown to proceed via an overall four-electron reduction pathway with a reaction order of one with respect to O_2. However once blockage of active sites occurs by adsorption or surface oxidation, the O_2 reduction reaction may deviate from the four-electron process.

5. ACKNOWLEGEMENTS

This research is funded under the Industrial Research Chair agreement between the Canadian Natural Sciences and Engineering Research Council (NSERC) and Ontario Power Generation (OPG), Toronto, Canada.

REFERENCE

---

[1] J. McMurry, D.A. Discon, J.D. Ikeda, S. Strois-Gascoyne, P. Baumgartner, and T.W. Melnyk. Ontario Power Generation Report No: 06819-REP-01200-10092-R00 (2003)

[2] D.W. Shoesmith, S. Sunder, W.H. Hocking, in J. Lipkowski, P.N. Ross, Electrochemistry of Novel Materials, VCH, New York, 1994, p297.

[3] W.H. Hocking, J.S. Betteridge, D.W. Shoesmith, J.Electroanalytical Chem., 379,339-351(1994).

[4] D.W. Shoesmith, W.H. Hocking, J.S. Betterdge, The influence of UO_2 fuel composition on its corrosion behavior under waster disposal conditions, Ontario Power Generation Report No:06819-REP-01200-10052-R00 (2001)

[5] V.A. Presnov, A.M. Trunov, Electrokhimiya 11, 77(1975).

[6] D.W. Shoesmith, J. Nucl. Mater., 282, 1-31(2000).

[7] E. Yeager, Electrochimica Acta, 29, 1527(1984)

[8] V.G. Levich, Physicochemical Hydrodynamics, Prentice Hall Inc., Englewood Cliffs, NJ, 1962

[9] A. Bonnel, F. Dabosi, C. Deslouis, M. Dupart, M. Kedam, B. Tribollet, J. Electrochem. Soc. 130, 753 (1982)

[10] C. Shi, F.C. Anson, Inorg. Chem., 31 (1990) 4298

[11] C.C. Chang, T.C. Wen, H.J. Tien, Electrochimica Acta, 42 (1997) 557-565.

[12] S.Lj. Gojkovic, S. Gupta, R.F. Savinell, J. Electroanalytical Chem., 462 (1999) 63-72.